Peptides 182 (2024) 171311

Contents lists available at ScienceDirect

Peptides

journal homepage: www.elsevier.com/locate/peptides

Membrane alteration, anti-virulence properties and metabolomic perturbation of a chionodracine-derived antimicrobial peptide, KHS-Cnd, on two bacteria models

Esther Imperlini [a,1], Federica Massaro [a,1], Angelica Grifoni [a], Francesco Maiurano [a], Anna Rita Taddei [b], Stefano Borocci [a,c], Francesco Buonocore [a,*], Fernando Porcelli [a]

[a] Department for Innovation in Biological, Agrofood and Forest Systems, University of Tuscia, Largo dell'Università snc, Viterbo, Italy
[b] Center of Large Equipments, Section of Electron Microscopy, University of Tuscia, Largo dell'Universit`a Snc, Viterbo 01100, Italy
[c] Institute for Biological Systems of Italian National Research Council (ISB-CNR), Secondary Office of Rome-Reaction Mechanisms c/o Department of Chemistry, La Sapienza University of Rome, Piazzale Aldo Moro 5, Rome 00185, Italy

ARTICLE INFO

Keywords:
Antimicrobial peptide
Anti-virulence
Protease
Extracellular protein
NMR-based metabolomics
Cytotoxicity

ABSTRACT

Antarctic fishes, living in an extreme environment and normally exposed to pathogens, are a promising source of antimicrobial peptides (AMPs). These are emerging as next-generation drugs due to their activity against multidrug resistant (MDR) bacteria. To infect hosts, beyond intrinsic/acquired resistance, MDR species also use virulence factors such as protease secretion. Hence, AMPs targeting virulence factors could represent a novel strategy to counteract the antimicrobial resistance (AMR). In this paper, we focused on a mutant peptide, named KHS-Cnd, that was obtained from the scaffold of the chionodracine (Cnd), a natural peptide identified in the icefish *Chionodraco hamatus*. We studied different effects caused by the peptide interaction with the cell membrane of two model bacteria, *E. coli* and *B. cereus*. First, we investigated its membranolytic activity revealing that the peptide action is more evident on *E. coli*, with a 69 % uptake of the used dye at 3 μM, whereas for *B. cereus* we found only a 65 % uptake at 6 μM. Successively, we determined the impact of this lysis on total protein concentration in the medium and an increase was estimated for both bacteria (84 % after 1 h for *E. coli* and 90 % for *B. cereus*, respectively). Moreover, we evaluated the changes in the proteolytic activity of the supernatant, that is an important aspect of bacterial resistance, showing that there was a significant reduction for both bacteria, although at higher level in the case of *E. coli*. The membranolytic activity was evidenced also morphologically with TEM analysis and a different alteration was evidenced for the two bacteria. Moreover, NMR metabolomics analysis showed that peptide induces changes in *E. coli* and *B. cereus* extracellular metabolites especially at the higher tested concentrations: this metabolic variation could be used as a fingerprinting of the peptide action on bacteria physiology due to its interaction with cell wall. Finally, we determined the KHS-Cnd cytotoxicity on human primary cell lines to verify its selectivity toward bacterial cell membranes and we found low toxicity until a concentration of 5 μM. Considering that the peptide exerts both membranolytic and anti-virulence activity on *E. coli* at 1.5 μM, we confirmed the interesting potential of this AMP as a new drug to counteract AMR.

1. Introduction

Antimicrobial resistance (AMR) in bacteria is a rapidly growing global public health concern. Different human bacterial pathogens over-exposed to pharmaceutical antibiotics have developed mechanisms of resistance rendering them ineffective and leading to an increased prevalence of infectious AMR diseases [1–3].

Given the rise of these multidrug-resistant (MDR) bacteria, new antimicrobial drugs and therapeutic approaches are urgently needed. In this context, antimicrobial peptides (AMPs) have been identified as potential next-generation antibiotics, since they are bioactive small peptides exhibiting broad spectrum of antimicrobial properties against a wide variety of bacteria, viruses, yeasts, and protozoa, and, surprisingly, also showing anticancer activity [4–7]. Hence AMPs, produced as

* Corresponding author.
E-mail address: fbuono@unitus.it (F. Buonocore).
[1] These two authors equally contributed to the paper.

https://doi.org/10.1016/j.peptides.2024.171311
Received 30 May 2024; Received in revised form 15 October 2024; Accepted 17 October 2024
Available online 18 October 2024

effectors of the innate immune responses by all living species, could also serve as antimicrobial agents showing several advantages over conventional antibiotics: rapid and broad spectrum of antimicrobial activities with potentially low toxicity for the host and low risk of developing antimicrobial resistance [4,8].

To date, several AMPs have been isolated from natural sources such as vertebrates and invertebrates, and others have been rationally designed and synthesized in laboratories. Based on the Antimicrobial Peptide Database (APD) reports, more than 3146 natural AMPs have been identified from various organisms, of which 383 from bacteria (i.e., bacteriocins), 5 from archaea, 8 from protists, 29 from fungi, 250 from plants, and 2463 from animals (https://aps.unmc.edu/, January 2024). APD database also contains 190 predicted and 314 synthetic AMPs with known antimicrobial activity.

Some of the natural AMPs have rather long mature sequences (up to 100 amino acid residues), which can compromise their pharmaceutical application due to their relatively challenging peptide synthesis and consequent high production cost, especially at an industrial scale, if compared to biologicals [9,10]. Hence, research is focusing on identifying natural peptide scaffolds as a base to develop new AMPs that are usually composed of 15–50 amino acids in their mature form and mostly cationic peptides with propensities to adopt α-helices and β-sheets structures [9,11,12].

To this aim, we focused on Antarctic marine organisms that are significant reservoirs of natural biomolecules [13]. We identified and characterized a piscidin-like AMP, named chionodracine (Cnd), from the Antarctic fish *Chionodraco hamatus* which was highly active against Antarctic psychrophilic bacteria and did not show hemolytic effect against human erythrocytes [14,15]. Starting from the natural Cnd peptide, different mutants were designed to improve its antibacterial activity against human pathogens [16]. Analogues were modified considering both the positive charge and the hydrophobic distribution of residues. Since the number of positive charges is crucial for the interaction with the negatively charged bacteria membrane and for the antimicrobial activity, we modified the wild-type Cnd by introducing lysines as charged residues. Specifically, Ser-11, Ser-22, and three Histidines in positions 4,15, and 17 have been replaced by lysines, increasing the charge from +2 to +7. Moreover, the mean charge for residue increased from ~0.09 to ~0.32, while the average number of hydrophobic residues was ~0.6, preserving the amphiphilicity of the helix. The *in silico* test performed with the Peptide Cutter tool (https://web.expasy.org/peptide_cutter/) showed that KHS-Cnd is more resistant to chymotrypsin-low specificity and less resistant to trypsin action with respect to the wild type.

Among the Cnd-mutants, KHS-Cnd showed the highest capacity to kill ESKAPE pathogens [17].

Recently, we tested the anti-virulence activity of KHS-Cnd against clinical *Pseudomonas aeruginosa* isolates from patients with cystic fibrosis. Our results showed that KHS-Cnd impaired biofilm formation and was also able to counteract the *Pseudomonas aeruginosa* invasion in pulmonary cells [18]. Considering our previous results, we decided to deeper investigate both the lytic and anti-virulence activity of this peptide against two model bacteria, the Gram-negative *Escherichia coli* and the Gram-positive *Bacillus cereus*. The bacteria responses to the peptide were analysed in the medium supernatants evaluating total protein content and protease production. These aspects were studied at peptide concentrations known to be active in relation to cell wall perturbation and at different time points as we know that the peptide has low stability. Moreover, for both bacteria, in the presence and absence of the peptide, we carried out, by ^{1}H NMR, a metabolomic comparison of extracellular metabolites to investigate the insurgence of metabolic modifications. In our approach, we do not want to identify all the present metabolites but, rather than, to reveal the fingerprint pattern correlated to the treatment with the AMP. In this way, the fingerprint may be used to detect changes induced by interaction of the peptide with the cell wall and therefore linked to its antimicrobial action. Finally, we investigated its cytotoxic activity on human cell lines to determine peptide selectivity at the concentrations able to induce bacterial alterations and, therefore, its potential as a new drug.

2. Materials and methods

2.1. Peptide

The peptide KHS-Cnd (WFGKLYRGITKVVKKVKGLLKG) was purchased by Caslo Aps (Caslo Aps Kongens, Lyngby, Denmark) with a purity of 98 %. The concentration of peptide's solutions was determined spectrophotometrically with a Jasco V-630 UV–VIS spectrophotometer (Jasco International Co Ltd's, Tokyo, Japan) by measuring the UV light absorption at 280 nm (ε_{280}=6990 M^{-1} cm^{-1}).

2.2. Bacterial strains and growth conditions

Escherichia coli (ATTC 25922) and *Bacillus cereus* (ATCC 10876) were grown in Luria Bertani (LB from Sigma Aldrich, Milan, Italy) medium under orbital shaking (150–160 rpm) at 37 °C and 35 °C, respectively.

2.3. Human cell cultures

The primary human fibroblast FB789 cell line was grown until near confluence in in Dulbecco's Modified Eagle Medium (DMEM) containing 10 % fetal bovine serum (FBS), 1 % glutamine, and 1 % penicillin-streptomycin (Sigma Aldrich) in an atmosphere of 5 % CO_2 at 37 °C. These cells were washed with saline phosphate buffer (PBS), detached by trypsin/EDTA, harvested and appropriately resuspended in PBS or fresh complete medium for membrane permeability and cytotoxicity assays, respectively.

2.4. Outer membrane permeability assay

The outer membrane permeability of peptide was assayed by measuring the uptake of the fluorescent probe 1-aminonaphthalene-8-sulfonic acid (ANS) in bacteria and human cells as previously described [16]. Briefly, three independent bacterial cell cultures were grown to the mid-log phase in LB medium and then centrifuged at 3000 rpm, washed and resuspended in PBS to achieve an OD_{600} of about 0.6.

In the case of human cells, two independent cell replicates were performed; cells were resuspended in PBS buffer to reach 5 $\times 10^{6}$ cells per mL before to start the test.

Different aliquot of KHS-Cnd peptide stock solution were added to 0.7 mL (peptide concentration from 0 to 30 μM) of cell suspension in presence of 25 μM ANS. Fluorescence spectra were recorded at wavelengths between 400 and 600 nm and reported in Supplemental Fig. 1 [19]. The increased permeability of the outer membrane was monitored by measuring the increase of fluorescence intensity due to the ANS probe incorporation into the membrane and calculated as follows [16]:

$$\% \text{ Uptake ANS} = (F - F_0)/F \text{ x}100$$

where F is the fluorescence of ANS observed at a given peptide concentration and F_0 is the fluorescence of ANS in the absence of peptide. The ANS uptake rates were reported in Supplemental Fig. 2.

2.5. Peptide treatment of bacteria

For KHS-Cnd treatment, each culture of exponentially growing *E. coli* and *B. cereus* bacteria (OD_{600} of 0.6) was split in three aliquots: two were treated with peptide at two different concentrations, and the other was left untreated (control). Specifically, KHS-Cnd peptide was added to *E. coli* cultures at the final concentrations of 1.5 μM and 3.0 μM, whereas 6.0 μM and 12 μM concentrations were used for *B. cereus* cultures. The

above concentrations were chosen after assaying the outer membrane permeability of the bacteria with the peptide (see Section 2.4).

For both bacteria (treated and control samples), the relative OD_{600} were measured each hour in the following 4 h after adding the peptide (Supplemental Fig. 3).

After different time points of peptide incubation, independent cell cultures of treated/untreated samples were centrifuged at 3600 rpm at 4 °C for 7 min. The KHS-Cnd treated/untreated culture supernatants of both bacterial strains were stored at 4 °C for use in the subsequent experiments. Bacterial cell cultures (control and treatments) were obtained from at least three independent replicates.

2.6. Protein assay

Protein concentrations were determined by using Bradford's reagent (from Biorad, Segrate, Italy). A standard curve based on bovine serum albumin (BSA) was employed, and analyses were carried out at a wavelength $\lambda = 595$ nm according to the manufacturer's protocol (Biorad). Protein content in the bacterial culture supernatants was expressed in mg and normalized to OD_{600}. Each experiment was performed at least in three independent replicates. As positive control, protein content was also determined in the supernatants of bacterial cells treated with 6 % v/v Triton X-100.

2.7. Protease assay

The total proteolytic activity was determined in the bacterial cultures by the azocasein assay, as previously described [18]. Briefly, 150 μL of KHS-Cnd treated or untreated culture supernatants were added to 500 μL of 0.3 % w/v azocasein (Sigma Aldrich) in 50 mM Tris–HCl, 0.5 mM $CaCl_2$ pH 7.5. After incubation at 37 °C for 30 min, an equal volume of l0 % v/v ice-cold trichloroacetic acid was added and incubated at 4 °C for 10 min to stop the enzymatic reaction. To remove the insoluble azocasein, samples were then centrifuged at 10000 rpm for 10 min, and the OD of the collected supernatants was measured at 400 nm. Each experiment was performed at least in triplicate.

2.8. Transmission electron microscopy (TEM)

Mid-log phase *E. coli* and *B. cereus* were treated with KHS-Cnd as described above (see Section 2.4) for 1 h and 2 h, respectively. The bacterial cultures without adding the peptide represented the negative controls, whereas those treated with 6 % Triton X-100 were used as positive controls. After peptide treatments, the bacteria were harvested by centrifugation at 3600 rpm at 4 °C for 14 min, washed three times with PBS, and fixed with 2 % paraformaldehyde and 2.5 % glutaraldehyde in 0.1 M cacodylate (Electron Microscopy Science) pH 7.2 at 4 °C for 3 h. After three washes with cacodylate buffer, the samples were post-fixed with 1 % osmium tetroxide (Electron Microscopy Science) in cacodylate buffer at 4 °C for 1 h. After other washes with cacodylate buffer, the samples were dehydrated in ethanol as previously described [19]. The dehydrated samples were transferred to mixtures of acrylic resin LRWhite (London Resin White) and ethanol at increasing concentrations of resin (v/v = 1/2, v/v = 1/1 and v/v = 2/1), 1 h for each step, and then to pure acrylic resin overnight. The sample embedding was carried out using hermetic gelatin capsules and the following polymerization was performed at 50 °C for 36 h. Ultrathin sections (60–80 nm thick) were then obtained by using an ultramicrotome, stained with uranyl acetate and lead citrate, and imaged by TEM (Jeol 1200 EX II TEM equipped with an Olympus SIS Veleta CCD camera and the iTEM software).

2.9. NMR spectroscopy analysis

2.9.1. Sample preparation

For NMR measurements, after growing, 3 mL of treated/untreated culture medium was evaporated in a vacuum centrifuge and, then dissolved in 600 μL of phosphate buffer 0.1 M, pH 7.0, containing 0.3 mM of 3-trimethylsilyl [2,2,3,3-d4] propanoic acid (TSP) sodium salt (Sigma, MO, USA) as the inner standard, and 10 % (v/v) of D_2O. Finally, 550 μL of this solution were transferred into 5 mm NMR tubes for NMR analysis.

2.9.2. Data acquisition

All one-dimensional ^1H NMR spectra were acquired on a Bruker Avance operating at 400 MHz (Bruker Biospin, Germany) at 25±1 °C. Tuning, matching, and shimming were carried out before each sample, and the 90° pulse length was calibrated on each sample. The 1D ^1H spectra were acquired using the standard Bruker pulse sequence *zgpr*, and water suppression was achieved using continuous wave irradiation. The spectral width was 11 ppm, and each spectrum was recorded using 128 transients, a relaxation delay of 3 s, an acquisition time of 4 s, and 32 k points. Free induction decays (FID) were zero-filled to 64 k data points and multiplied by an exponential function equivalent to 0.3 Hz line broadening before Fourier transformation. The transformed spectra were referenced to TSP resonance at 0.0 ppm and manually corrected for phase and baseline. Then, the spectra were reduced into spectral bins of 0.02 ppm using the ACD intelligent bucketing method (^1D NMR Manager software ACD/Labs, Toronto, Canada), excluding the residual water region δ 4.54–5.22 and the TSP peak δ −0.5–0.5.

2.9.3. NMR data analysis

All NMR experiments were conducted in six replicates for *E. coli* and 4 replicates for *B. cereus*. NMR spectra of medium samples were represented by 355 bins corresponding to a range of chemical shifts in ppm, integrated and transformed into a comma-delineated form (CSV) for statistical analysis with the Metaboanalyst 6.0 software (http://www.metaboanalyst.ca). The data were standardized using normalization by sum, square root transformation and Pareto scaling which are present in Metaboanalyst. Partial Least Squares Discriminant Analysis (PLS-DA) was applied to maximize the separation between the groups and to obtain a better prediction of the variables. The most relevant ^1H NMR variables (the metabolites) sensitive to the AMP treatment were identified using the VIP (variable importance in projection) scores with VIP > 1 and $p < 0.05$. Metabolites were identified using Chenomx NMR Suite 10.0 and an in-house NMR database and they are reported in Supplemental Fig. 4 and Fig. 5.

2.10. Cytotoxicity assay against human cell line

The cytotoxicity of KHS-Cnd peptide was tested on primary human FB789 fibroblasts grown as reported above. Cells were seeded on 96-well microplates at a density of 10^4 cells per well in 100 μL of the medium overnight. Then, four peptide dilutions (1.5, 3.0, 6.0 and 12 μM) were added to the cells that were incubated at 37°C under 5 % CO_2 for 3 h or 24 h. Cells grown in normal medium without peptide but added with an equal amount of water were used as a negative control, while, as a positive control, cells were treated with 2 % NaN_3.

The cell viability was assayed by using the 3-(4,5-dimethylthiazol-2-yl)-2,5-diphenyl-2H-tetrazolium bromide (MTT) dye as previously described [20]. In each well, the culture medium was removed and replaced with fresh medium containing 0.5 mg/mL MTT and then incubated at 37 °C in a 5 % CO_2 atmosphere for 3 h. After removing the cell medium, the purple crystal formazan was dissolved in 100 μL of dimethyl sulfoxide (DMSO) and incubated at 37 °C for 15 min. The absorbance at 595 nm was measured on a Epoch2 microplate spectrophotometer (BioTech). Cell viability was expressed as the percentage of viable cells in the presence of different KHS-Cnd concentrations compared to the negative control. Each experiment was performed at least in two independent replicates.

2.11. Statistical analysis

Data were presented as mean ± standard deviation (SD). The Student's *t*-test was performed for comparison between two groups. The significance difference threshold was $p < 0.05$.

3. Results

3.1. Membranolytic activity of KHS-Cnd peptide

To evaluate the permeabilizing effect of KHS-Cnd peptide on the outer membrane of Gram-negative *Escherichia coli* bacterium and on the plasmatic membrane of Gram-positive *Bacillus cereus* bacterium, we performed a fluorescence assay using the ANS probe. The ANS fluorescence is very weak in an aqueous medium, but it turns to high values in a hydrophobic environment. Hence, in presence of intact bacterial cells, there is a very weak fluorescence emission; upon perturbation/disruption of the cell membrane, the ANS is able to penetrate into the lipid bilayer, thus leading to a drastic increase in ANS fluorescence intensity [21].

In Fig. 1 it has been reported the percentages of ANS uptake for the permeabilization of *E. coli* and *B. cereus* upon addition of increasing concentrations of KHS-Cnd peptide. The rapid increase in ANS fluorescence indicated that KHS-Cnd perturbs both the outer membrane of *E. coli* and the plasmatic membrane of *B. cereus*, but at different peptide concentrations. For the Gram-negative bacteria, the ANS uptake was 55 % and 69 % at 1.5 μM and 3.0 μM of KHS-Cnd, respectively (Fig. 1). For the Gram-positive bacteria, instead, the ANS uptake was 65 % and 76 % at 6.0 μM and 12 μM of KHS-Cnd, respectively (Fig. 1). Hence, the membranolytic activity of KHS-Cnd is higher against *E. coli* compared to the effect observed for *B. cereus*.

Preliminary experiments were carried out to assess the effect of KHS-Cnd on the number of *E. coli* and *B. cereus* cells determined reading OD values at peptide concentrations known to produce membranolytic activity on the bacteria. We treated exponentially growing ($OD_{600\ nm}$ of 0.6) *E. coli* and *B. cereus* cultures with 1.5 μM and 6.0 μM KHS-Cnd, respectively, as they represent the respective concentrations at which the ANS probe showed a similar uptake for both bacteria (Fig. 1). We also treated both bacteria with a 2-fold peptide concentration, namely *E. coli* with 3.0 μM KHS-Cnd and *B. cereus* with 12 μM KHS-Cnd to investigate a dose-dependent effect. As shown in Supplemental Fig. 3 A,

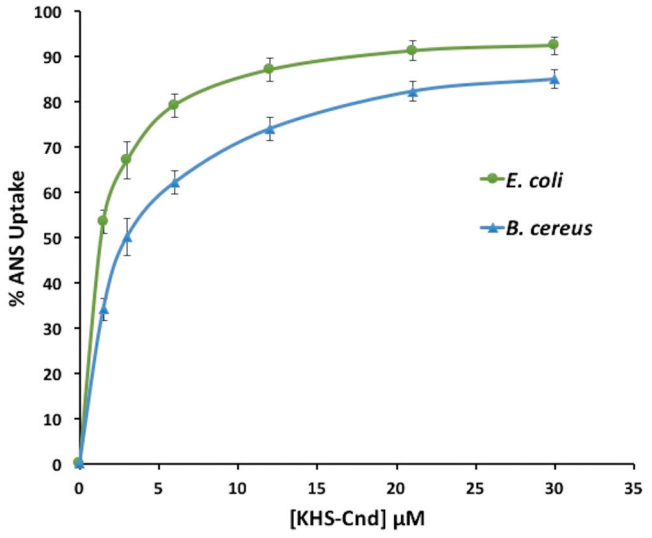

Fig. 1. Permeabilizing effect of KHS-Cnd peptide on *E. coli* outer membrane and *B. cereus* plasma membrane. Percentage of ANS uptake as a function of peptide concentration. Values represent mean ± SD of three independent experiments performed at least in duplicates.

the peptide, at both 1.5 μM and 3.0 μM concentrations, did not affect *E. coli* duplication rate. Different results were obtained evaluating the effect of KHS-Cnd on the *B. cereus* OD rate (Supplemental Fig. 3B): upon addition of 12 μM KHS-Cnd, *B. cereus* strain showed a significantly decreased rate, particularly at 1 h, 2 h and 3 h after treatment in comparison to untreated cells (control). However, at 4 h after the addition of KHS-Cnd, there is no difference in the OD rate of *E. coli* and of *B. cereus* between treated and control cells; this could indicate a rapid kinetics of action of the peptide within 1–3 h, as evidenced also by our subsequent analyses.

3.2. Determination of protein content in bacterial culture supernatants after KHS-Cnd peptide treatment

To determine the impact of the membranolytic activity of KHS-Cnd peptide on the two model Gram-negative/positive bacteria, we estimated the total extracellular proteins using the Bradford assay. Based on the evaluation of bacterial OD after peptide treatment, protein content in the culture supernatants was assessed within 1–3 h after treatment with KHS-Cnd peptide at the selected concentrations. When the protein content was assayed in the *E. coli* culture supernatants, a statistically significant increase was observed after the treatment with 3.0 μM KHS-Cnd (Table 1). In particular, 1 h after exposure to this concentration, we found that protein content significantly increased by 84 % in the *E. coli* culture supernatants compared to the control; however, a significant increase of 47 % was still observed after 3 h of the treatment with 3.0 μM KHS-Cnd (Table 1).

As reported in Table 2, a statistically significant increase of about 90 % was assayed in the *B. cereus* culture supernatants at 1 h and 2 h after the treatment with 12 μM KHS-Cnd.

As positive control we used 6 % Triton X-100, a commonly used membrane-disrupting agent. This led to a strong rupture with a formation of leaky membranes as evidenced by the protein releases in the culture supernatants that were very consistent for both bacteria if compared with untreated cells; notably, for each strain, the high protein contents were similar at both time points of treatment with Triton X-100 (Tables 1 and 2).

3.3. Effect of KHS-Cnd peptide on protease activity

Since bacterial proteases play different roles in cell physiology, infection pathogenesis and bacterial AMP resistance, we decided to investigate the proteolytic activity, by using azocasein assay, in the culture supernatants of *E. coli* and *B. cereus*, within 1–3 h from the treatment with KHS-Cnd peptide at the previous selected concentrations (Fig. 2). A significant reduction (32–42 %) in protease activity was observed in the supernatants of *E. coli* after 1 h of treatment with both considered KHS-Cnd concentrations in comparison to the control (Fig. 2A). Moreover, a significant reduction in protease activity was also highlighted 3 h after the peptide treatments, albeit to a lesser extent (Fig. 2A).

B. cereus showed a significant protease activity reduction after 1 h of

Table 1
Protein content in *E. coli* culture supernatants at 1 h and 3 h after treatments with 1.5 μM or 3.0 μM KHS-Cnd.

E. coli	**mg/$OD_{600\ nm}$**	
	1 h	**3 h**
Control	0.163±0.019	0.161±0.024
1.5 μM KHS-Cnd	0.236±0.047	0.187±0.025
3.0 μM KHS-Cnd	0.300±0.030**	0.237±0.009*
6 % Triton X−100	14.8±0.6	16.4±3.6

mg of protein content normalized to $OD_{600\ nm}$ represents mean ± SD of three independent experiments performed in triplicates.
* = $p < 0.05$, ** = $p < 0.005$ compared to the control.

Table 2
Protein content in *B. cereus* culture supernatants at 1 h and 2 h after treatments with 6.0 μM or 12 μM KHS-Cnd.

B. cereus	mg/$OD_{600\ nm}$	
	1 h	2 h
Control	0.209±0.035	0.127±0.025
6.0 μM KHS-Cnd	0.266±0.032	0.178±0.050
12 μM KHS-Cnd	0.395±0.053*	0.243±0.052*
6 % Triton X−100	37.1±1.8	35.5±6.2

mg of protein content normalized to $OD_{600\ nm}$ represents mean ± SD of three independent experiments performed in triplicates.
* = $p < 0.05$ compared to the control.

exposure only at the concentration of 12 μM of KHS-Cnd compared to the control (Fig. 2B). Furthermore, after 2 h of treatment the reduction was significant for both selected concentrations, not exceeding values of about 30 % (Fig. 2B).

3.4. Assessment of morphological and ultrastructural changes in bacterial cells after KHS-Cnd peptide treatment

Ultrastructural morphology of bacterial cells treated with KHS-Cnd peptide was observed using transmission electron microscopy (TEM). TEM micrographs of untreated *E. coli* and *B. cereus* control cells (Fig. 3A and Fig. 3E, respectively) showed: i) an intact surface with well-defined cell walls and membranes; ii) an electron-dense cytoplasm region compactly distributed around a central area with less density where

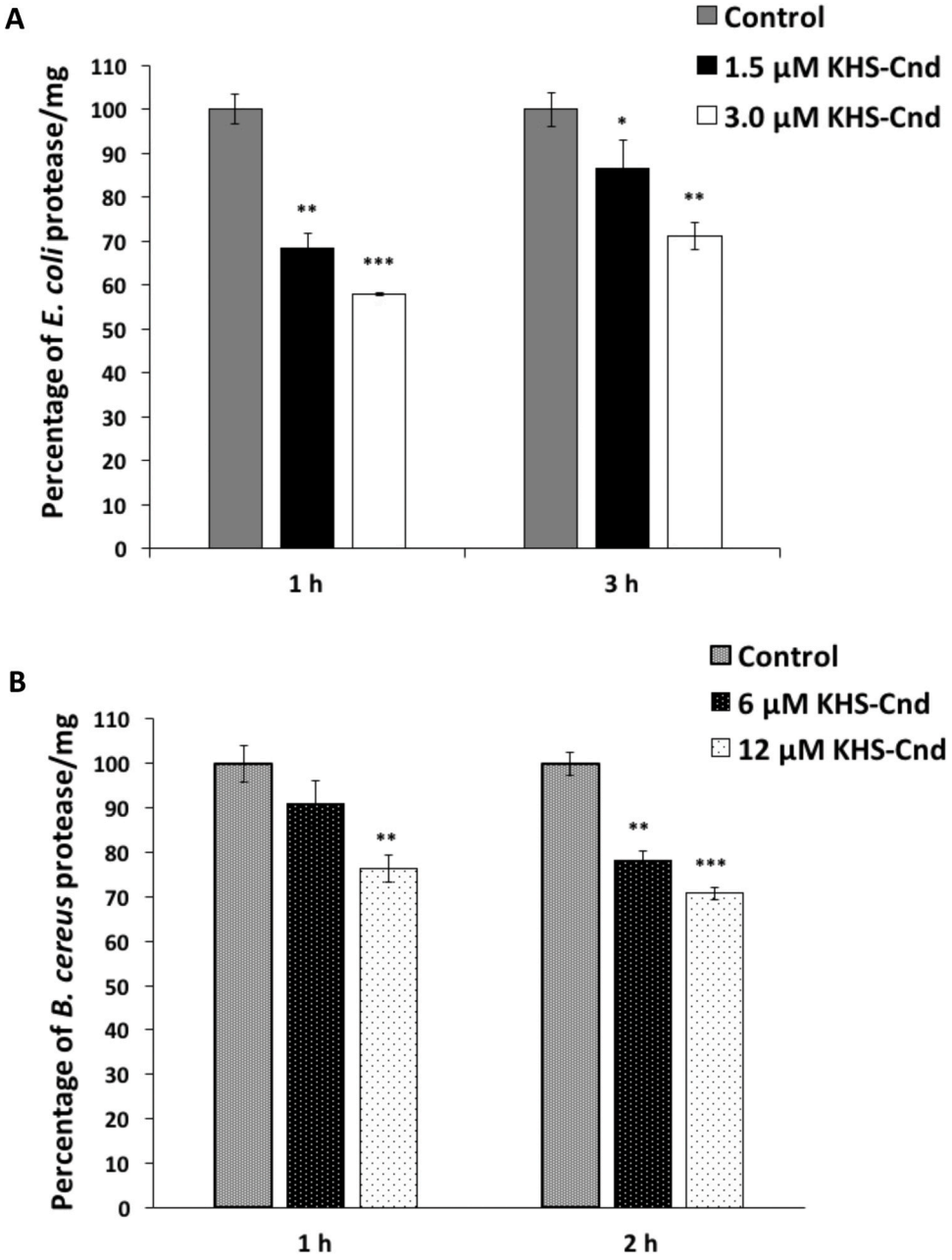

Fig. 2. Effect of KHS-Cnd peptide on the protease activity of bacterial supernatants. A) Proteolytic activity assayed in the *E. coli* culture supernatants after 1 h and 3 h treatment with 1.5 μM and 3.0 μM KHS-Cnd. B) Proteolytic activity assayed in the *B. cereus* culture supernatants after 1 h and 2 h treatment with 6.0 μM and 12 μM KHS-Cnd. Data are expressed as percentage of residual proteolytic activity (normalized to mg of protein) compared to the control (untreated cells). Values represent mean ± SD of three independent experiments performed in duplicates. * = $p < 0.05$, ** = $p < 0.005$, *** = $p < 0.0001$ compared to the control.

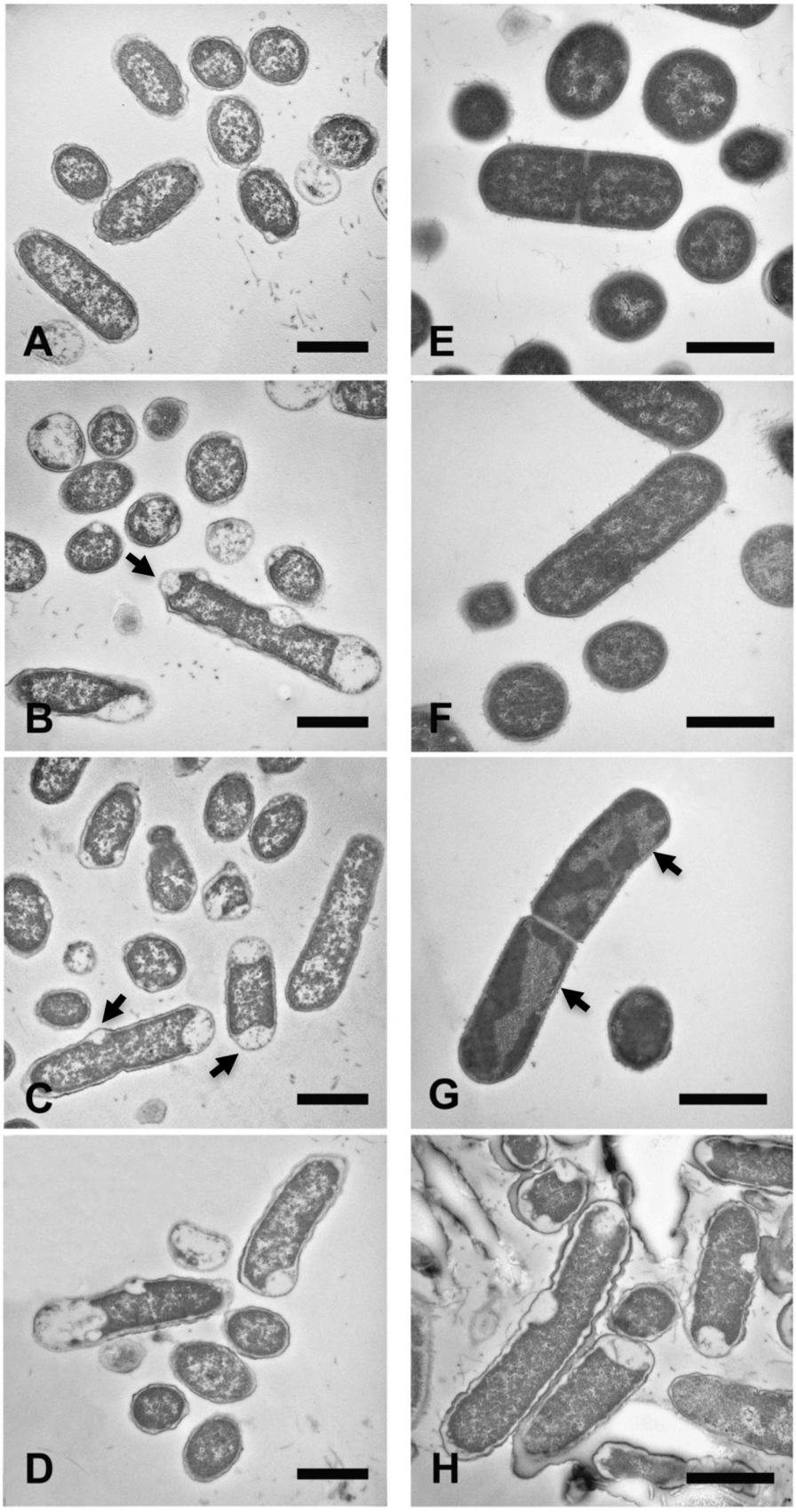

Fig. 3. TEM micrographs of bacteria treated with KHS-Cnd peptide. A) Untreated *E. coli* (control). B) *E. coli* treated with 1.5 μM KHS-Cnd for 1 h. C) *E. coli* treated with 3.0 μM KHS-Cnd for 1 h. D) *E. coli* treated with 6 % Triton X-100 for 1 h (positive control). E) Untreated *B. cereus* (control). F) *B. cereus* treated with 6.0 μM KHS-Cnd for 2 h. G) *B. cereus* treated with 12 μM KHS-Cnd for 2 h. H) *B. cereus* treated with 6 % Triton X-100 for 2 h (positive control). Scale bars represent 1 μm for A-D and 2 μm for E-H.

intracellular DNA is located.

The exposure of *E. coli* to KHS-Cnd peptide induced locally outer membrane disruption, DNA intracellular spread, and loss of cytoplasmic content as revealed by translucent zones (Fig. 3B and Fig. 3C). Moreover, in *E. coli* treated with both KHS-Cnd concentrations, it was possible to observe the appearance of some vacuoles (black arrows, Fig. 3B and Fig. 3C) that were also evident for the positive control represented by bacterial cells treated with the membrane permeabilizing non-ionic detergent Triton X-100 (Fig. 3D).

On the other hand, the exposure of *B. cereus* to KHS-Cnd did not induce the consistent membrane damage observed in *E. coli*. Similar to untreated control cells (Fig. 3E), TEM images showed the presence of an intact/resistant cell wall in treated bacteria (Fig. 3F and Fig. 3G). Despite this, a loss of intracellular content, including DNA and

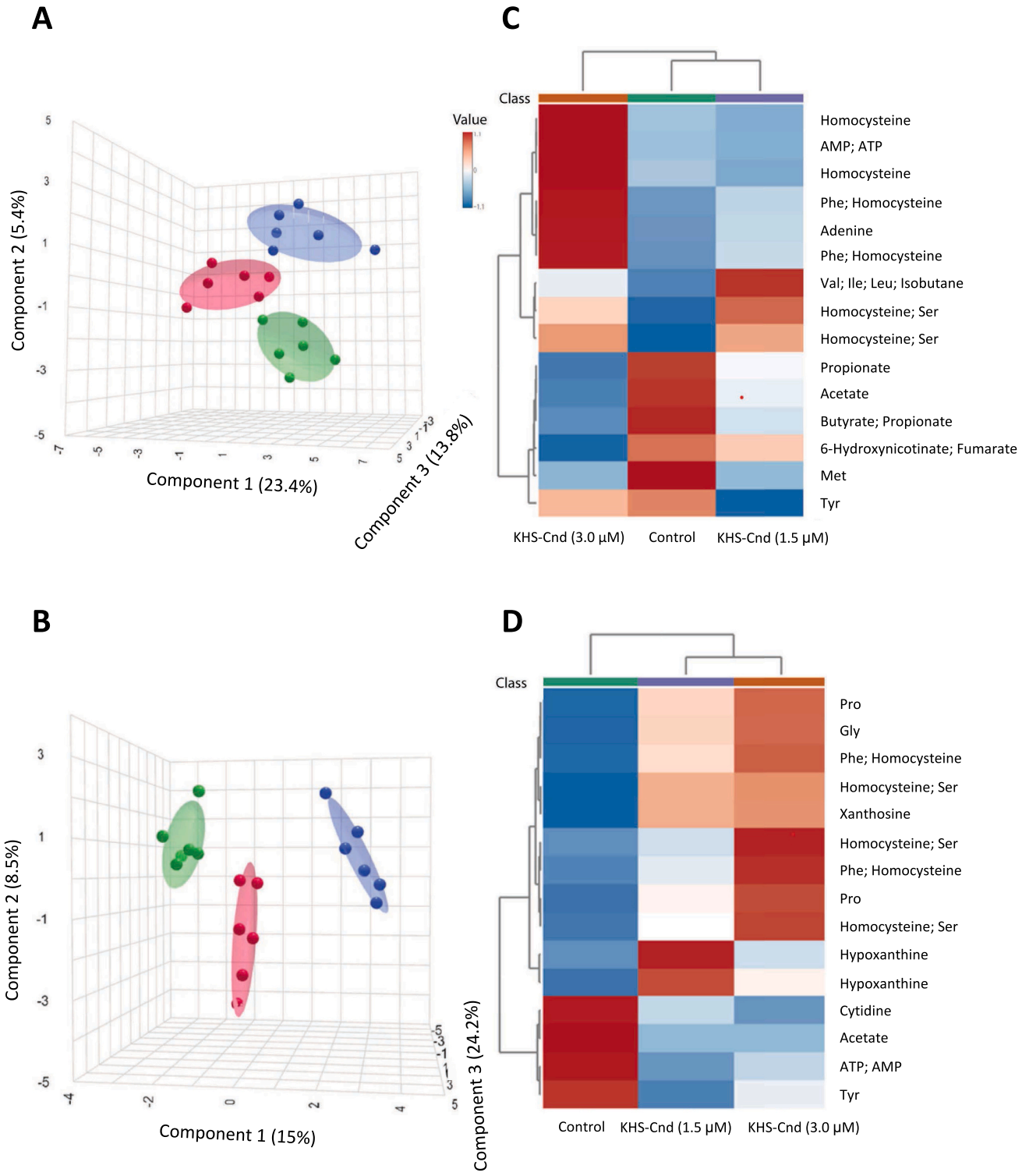

Fig. 4. Effect of KHS-Cnd peptide on *E. coli* extracellular metabolite profiles. A) and B) 3D PLS-DA score-plot of extracellular metabolic profile of untreated *E. coli* (control in blue), *E. coli* treated with 1.5 µM KHS-Cnd (red) and 3.0 µM KHS-Cnd (green) for A) 1 h and B) 3 h. C) and D) Heatmap visualization of extracellular metabolite relative abundance in untreated *E. coli* (control), *E. coli* treated with 1.5 µM KHS-Cnd and 3.0 µM KHS-Cnd) for C) 1 h and D) 3 h.

translucent zones were visible after peptide exposure to the highest concentration used for the Gram-positive bacterium (black arrows, Fig. 3G). Anyhow, these membrane ultrastructural changes were not comparable with those of the positive controls (Fig. 3H), whose morphological alterations were more evident if compared to the untreated cells (Fig. 3E).

3.5. Analysis of metabolites in E. coli culture supernatants after KHS-Cnd peptide treatment

To investigate the impact of different treatments on the extracellular *E. coli* metabolic profile, we studied the extracellular medium after 1 h and 3 h of treatment with the peptide at concentrations of 1.5 and 3.0 μM. The typical ^{1}H NMR spectrum of extracellular metabolites of *E. coli* is reported in Supplemental Fig. 4 with the 50 principally identified metabolites. Since metabolites usually contain more than one resonance signal, the resonance signals in overlapping regions can be resolved using equivalent signals in other regions. We analyzed the influence of treatments on metabolite profiles using PLS-DA (Partial Least Squares Discriminant Analysis). The comparison between *E. coli* untreated sample (Control) and different treatments (1.5 μM KHS-Cnd and 3.0 μM KHS-Cnd) showed a separation at 1 h and 3 h (Fig. 4A and Fig. 4B). Three major components after 1 h and 3 h are responsible for 23.4 %, 13.8 % and 5.4 %, and for 24.2 %, 15.0 %, 8.5 % of the total variance, respectively (Fig. 4A and Fig. 4B).

As reported in Fig. 4C and Fig. 4D, we used a heatmap to evaluate and visualize the change in the relative abundance of the 15 most representative metabolites.

Overall, the heatmaps showed an extracellular metabolic change in response to the addition of KHS-Cnd peptide, depending on the treatment time. Interestingly, the comparison between untreated *E. coli* (control) and treated with 3.0 μM KHS-Cnd allowed us to identify two dense groups of extracellular metabolites that showed a marked opposite relative abundance at each treatment time (Fig. 4C and Fig. 4D). As an example, we found that homocysteine is more represented in the bacterial supernatants of *E. coli* treated with 3.0 μM KHS-Cnd than in the control after 1 h and 3 h. In contrast, acetate is less represented in this treated sample compared to the control at both treatment times.

Then, we carried out the supervised OPLS-DA analysis to compare pairwise the changes observed in extracellular metabolic profiles of the control and 3.0 μM KHS-Cnd-treated samples at 1 h (Q^2=0.475, p=0.03; R^2=0.96 p<0.01) and 3 h (Q^2=0.86, p<0.01; R^2=0.98, p<0.01). In Fig. 5A and Fig. 5B, the VIP values of the 15 most important metabolites, such as homocysteine, Ser, Gly, Phe, acetate N-acetylglucosamine, and cystathionine, and their relative abundances are represented at 1 h and 3 h treatment with 3.0 μM KHS-Cnd, respectively. Fig. 5 indicates that the score plot differentiates the treated and control groups underlying an effect at the metabolic level. The metabolites involved in this discrimination were identified based on VIP values. Also, this analysis showed that the changes in the highlighted metabolites depend on the treatment time. Collectively, these analyses showed that the ^{1}H NMR-based metabolomic approach reflected the metabolic changes related to the stressful event caused by the addition of peptide.

3.6. Analysis of metabolites in B. cereus culture supernatants after KHS-Cnd peptide treatment

To investigate the impact of different treatments on the extracellular *B. cereus* metabolic profile, we studied the extracellular medium after 2 h of treatment with peptide at concentrations of 6.0 and 12 μM. We analyzed the influence of treatments on metabolite profiles using PLS-DA (Partial Least Squares Discriminant Analysis), as before. The comparison between *B. cereus* untreated sample (Control) and different treatments (6.0 μM KHS-Cnd and 12 μM KHS-Cnd) showed a separation (Fig. 6A). Three major components after 2 h are responsible for 23.6 %, 12.1 % and 10.5 %, of the total variance, respectively (Fig. 6A).

As reported in Fig. 6B, also for *B. cereus,* we used a heatmap to evaluate and visualize the change in the relative abundance of the 15 most representative metabolites. As for *E. coli*, the heatmap showed an extracellular metabolic variation upon treatment with KHS-Cnd at the two concentrations. Upon treatment, we can identify two groups of metabolites that show a gradual change of relative abundance depending on the peptide concentration (Fig. 6B). Specifically, we detected a gradual decrease of amino acids and betaine, and an increase of aromatic amino acids and cis-aconitate. The VIP values of the 15 most important metabolites, such as Ala, acetate, betaine GTP, $NADP^+$, Thr, lactate, homocysteine, 2'-hidroxyisobutyrate, Asp, oxo-valerate and their relative abundances are represented in Fig. 7 for the control and 6.0 μM and 12 μM of KHS-Cnd, respectively.

Collectively, these analyses showed that the ^{1}H NMR-based metabolomic approach can reveal, as already observed for *E. coli*, the metabolic changes consequent to the stressful event caused by the addition of the peptide.

3.7. Effect of KHS-Cnd peptide on membrane permeability and viability of human normal cells

The membranolytic activity of KHS-Cnd peptide was assessed on primary human fibroblast (FB789) cell line by measuring the uptake of ANS fluorescent at increasing concentrations of KHS-Cnd peptide (Fig. 8A). An induced dose-dependent increase of ANS fluorescence in human fibroblasts was observed. However, at 1.5–6 μM, the peptide only caused poor probe internalization, which did not exceed 28 %. At the highest concentration (12 μM) tested against bacteria, instead, the ANS uptake reached 42 % in human cells (Fig. 8A).

Moreover, we also investigated the cytotoxicity of KHS-Cnd peptide on FB789 fibroblasts. The cell viability was detected after 3 h and 24 h of incubation with the peptide at four different concentrations (1.5, 3.0, 6.0 and 12 μM). As shown in Fig. 8B, a very slight or negligible cytotoxic effect was found at the peptide concentrations tested against *E. coli* (1.5 and 3.0 μM) and *B. cereus* (6.0 μM). At these conditions, after 3 h and 24 h, the percentages of viable cells ranged from 76 % to 82 % compared to the untreated negative control cells (neg control). On the other hand, toxicity was observed for the highest concentration (12 μM) tested against *B. cereus*, for which a 30 % and 54 % of cell viability was observed after 3 h and 24 h, respectively.

4. Discussion

Antarctic fishes, living in an extreme environment, are a promising source for antimicrobial peptides (AMPs), that are fundamental components of the innate immune responses of these vertebrates [9]. These natural peptides are emerging as next-generation therapeutics due to their action against bacteria, viruses, yeasts and protozoa. As they show a broad spectrum of activity against multidrug-resistant (MDR) bacteria, strong efforts are being made to bring AMPs into clinical use, in order to counteract the increasing resistance to classical antibiotics. Beyond intrinsic/acquired resistance to infect hosts, MDR species also use virulence factors, like biofilm formation, motility, toxin, and protease secretion [22]. Bacterial proteases are physiologically necessary for cell replication and division, involved in the regulation of stress responses and required to increase bacterial virulence in many pathogenic strains [23]. Bacteria have developed specific protease secretion systems that enable them to adapt and survive in hostile environmental conditions [22]. In particular, bacterial proteases, secreted across the phospholipid membranes, enhance bacterial adhesion and invasion of eukaryotic cells, damage tissues and escape the host immune response [23,24]. The role of secreted proteases in bacterial virulence makes them suitable, so far underexploited, targets for the development of new antimicrobial/anti-virulence drugs. Hence, there is a need for innovative approaches targeting these virulence factors, especially in the case of bacteria involved in chronic pathogenesis.

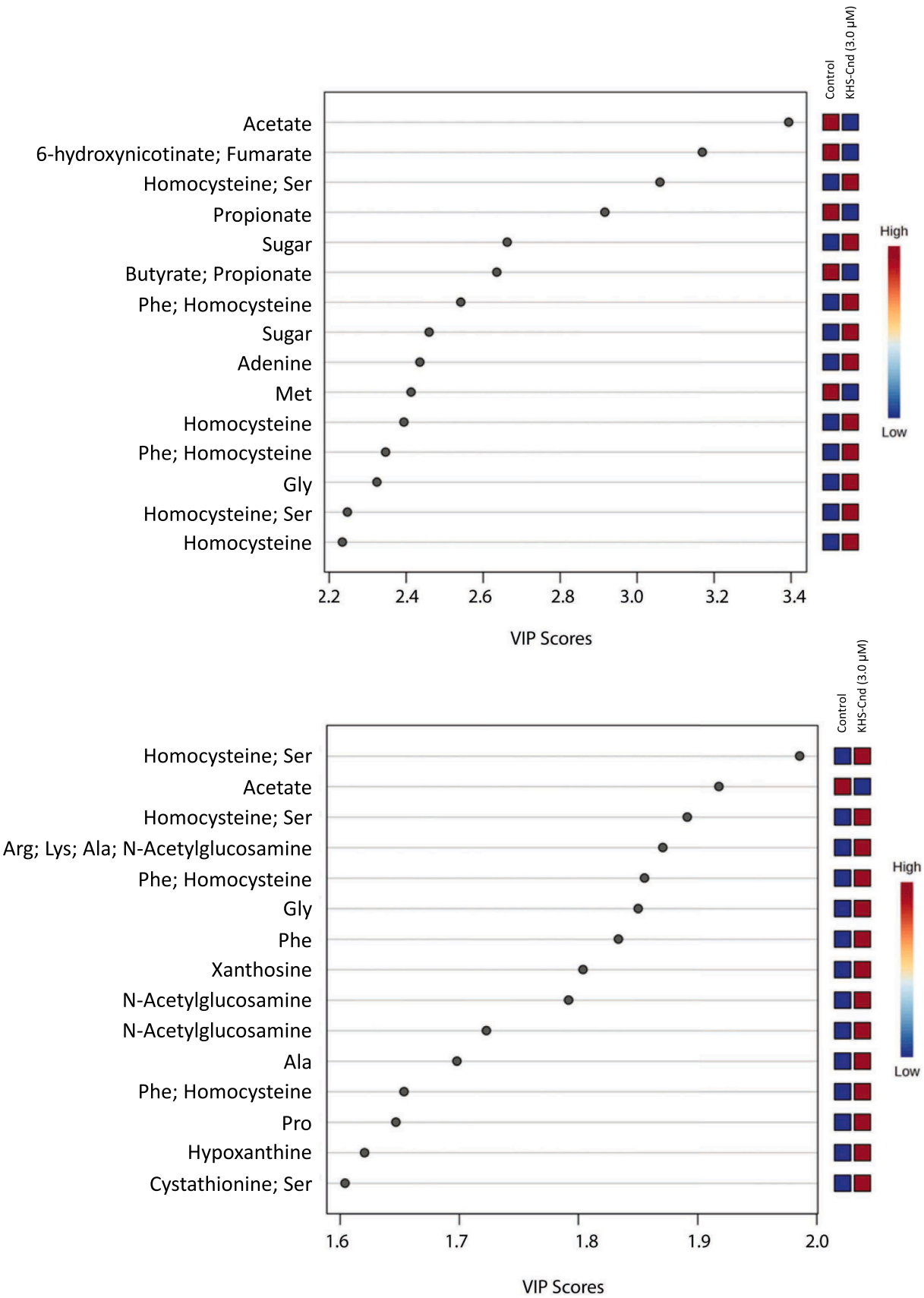

Fig. 5. Differential extracellular metabolite analysis after *E. coli* treatment with 3.0 μM KHS-Cnd peptide. VIP values of the 15 most important extracellular metabolites in untreated *E. coli* (control) and *E. coli* treated with 3.0 μM KHS-Cnd for A) 1 h and B) 3 h ($p < 0.05$).

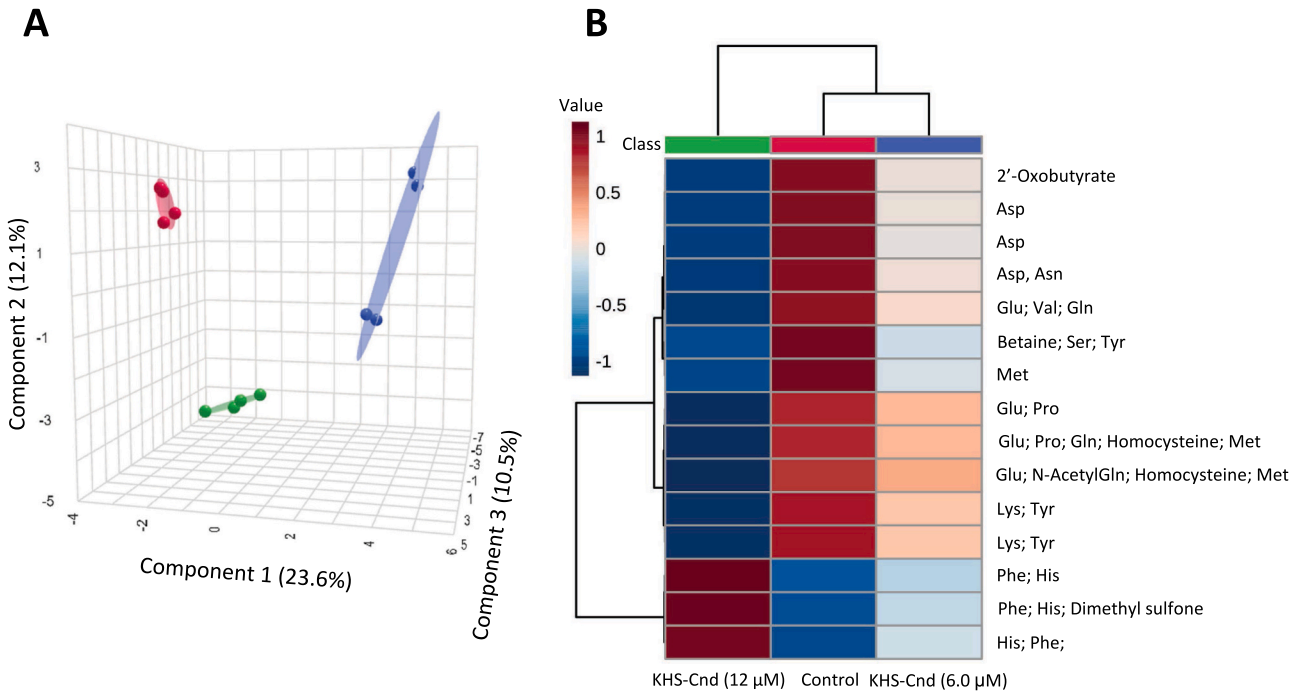

Fig. 6. Effect of KHS-Cnd peptide on *B. cereus* extracellular metabolite profiles. A) 3D PLS-DA score-plot of extracellular metabolic profile of untreated *B. cereus* (control in red), *B. cereus* treated with 6.0 μM KHS-Cnd (blue) and 12 μM KHS-Cnd (green) for 2 h. B) Heatmap visualization of extracellular metabolite relative abundance in untreated *B. cereus* (control), *B. cereus* treated with 6.0 μM KHS-Cnd and 12 μM KHS-Cnd) for 2 h.

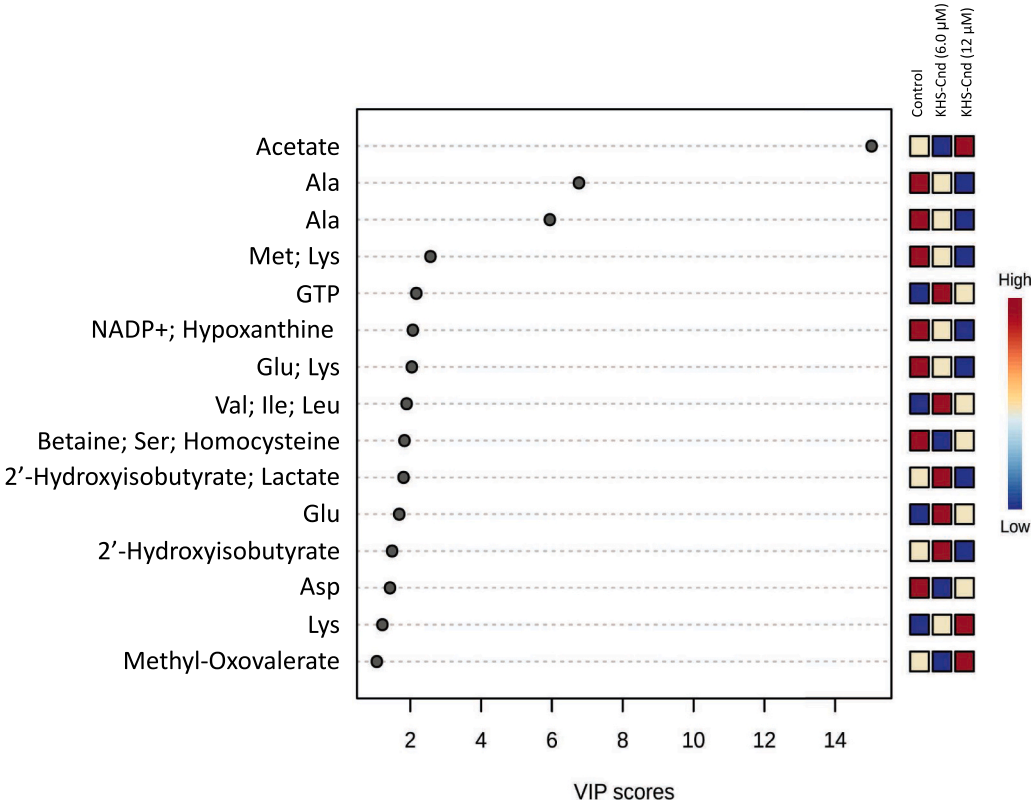

Fig. 7. Differential extracellular metabolite analysis after *B. cereus* treatment with 6.0 μM and 12 μM KHS-Cnd peptide. VIP values of the 15 most important extracellular metabolites in untreated *E. coli* (control) and *E. coli* treated with 6.0 μM and 12 μM KHS-Cnd for 2 h ($p < 0.05$).

In this study, we used a mutant peptide, named KHS-Cnd [16], designed from the scaffold of the chionodracine (Cnd), a natural peptide identified in the icefish *Chionodraco hamatus* [14]. Hence, we investigated, at the beginning, the membranolytic activity of KHS-Cnd peptide and its effect on some virulence factors, like total protein and protease production, of two models of Gram-negative/positive bacteria,

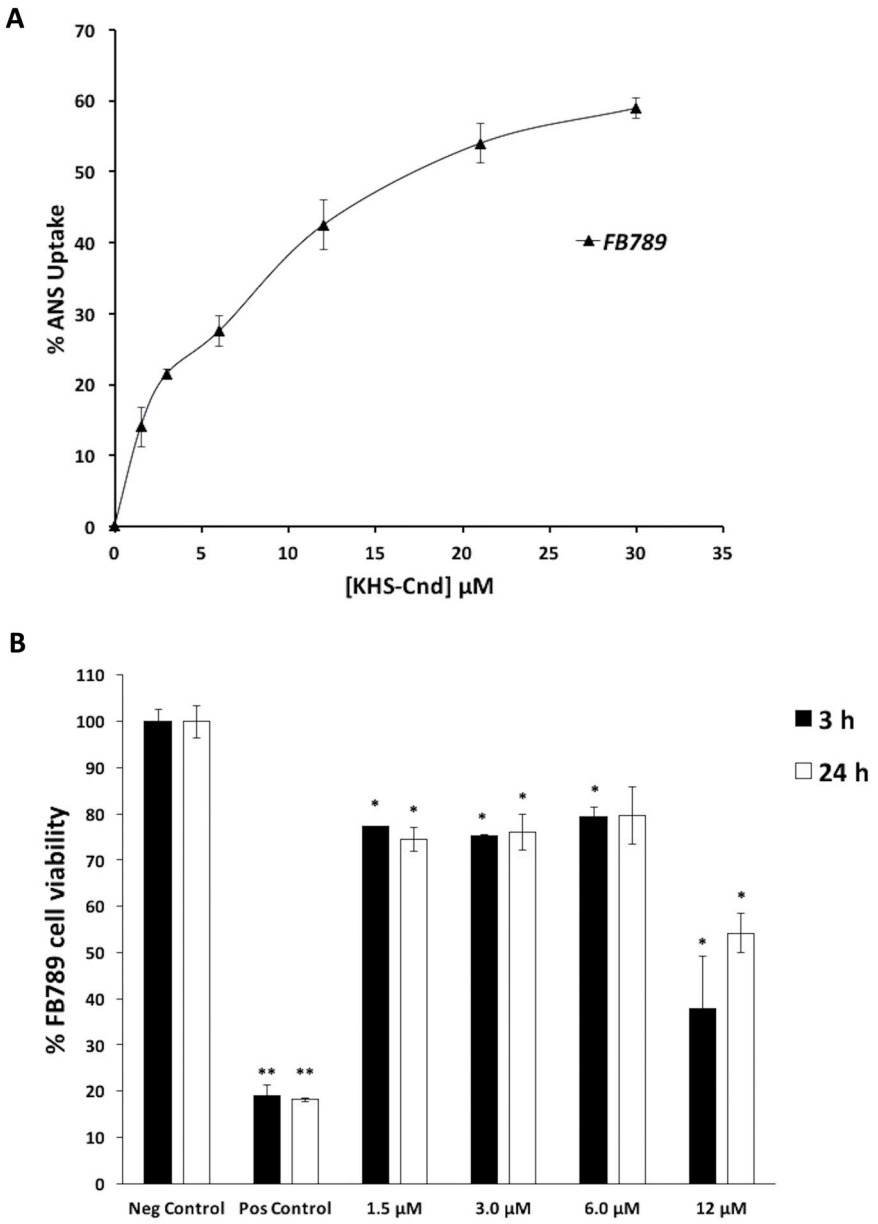

Fig. 8. Effect of KHS-Cnd peptide on the primary human fibroblast FB789 cell line. A) Percentage of ANS uptake in FB789 cells as a function of peptide concentration. Values represent mean ± SD of two independent experiments. B) Dose-response plot of cell viability, assessed by MTT assay, after 3 h and 24 h of incubation with increasing concentrations (1.5–12 μM) of peptide. As a negative control (Neg control), cells were grown in normal medium without peptide, while, as a positive control (Pos control), cells were treated with 2 % NaN_3. Values representing the percentage of viable cells relatively to the negative controls, were expressed as mean ± SD of two independent replicates (with 5 repeats for each replicate). * = $p < 0.05$, ** = $p < 0.005$ compared to the negative control.

Escherichia coli and *Bacillus cereus* respectively. The membranolytic assay gave the possibility to highlight the cell wall perturbation due to the peptide activity and to determine the specific peptide concentration needed to obtain the same detrimental effect on both bacteria. Interestingly, the concentration values selected for *E. coli* were close to the minimum inhibitory concentrations (MICs) and 2x MICs previously determined for the peptide [16]. To explore the mechanistic aspects of KHS-Cnd activity as well as its potential therapeutic use, we treated exponentially growing *E. coli* and *B. cereus* cultures and investigated the peptide effect on membrane perturbation, extracellular metabolite alterations and secreted virulence factors within 1–3 h from the treatment; in this experimental condition, we observed multiple effects resulting from the interaction of the peptide with cell membranes, but we are not able to appreciate any effect of KHS-Cnd on the bacteria growth curves. In this regard, experimental evidence showed that the concentration of free peptide as well as the number of cell-associated peptide molecules are key factors to induce an antibacterial effect [25]. On the other hand, MICs, determined using a standard bacterial density, often resulted ineffective to clinically treat the high-density infections [26]. In this scenario, the inhibition of virulence factors and the eliciting of physiological modification rather than bacterial viability could represent a promising strategy for the development of new antimicrobial drugs. Therefore, an AMP that shows these interesting properties with a good selectivity, testified by the low cytotoxicity and hemolytic activity, could still be interesting for a therapeutic use.

Moreover, as confirmed by TEM analysis, the treatment with peptide leads to membrane perturbation/alteration according to the possible mechanisms of AMPs action elsewhere described [4]. The morphological/ultrastructural results were supported by biochemical assays that highlighted an increased protein content in the bacterial culture

supernatants after KHS-Cnd peptide treatment. In fact, this reinforces the concept that the interaction of the cationic KHS-Cnd peptide with bacterial membranes leads to their depolarization with the leakage of intracellular material such as proteins and metabolites, and the consequent cell lysis. However, we cannot rule out that membrane damage is the starter mechanism of AMP action [4]. It's known that bacteria have developed specific mechanisms to respond against stress, including protein production/secretion, and that antimicrobial agents like AMPs represent one of unfavorable conditions for bacteria [27]. In addition to these mechanisms, the increase of protein content in the medium could be also due to the peptide entering into the cytoplasm, where it can target key bacterial processes including *de novo* protein synthesis as well as enzymatic activity such as proteolytic one. The rise in total mg of protein in the medium supernatant was greater after 1 h from the treatment with *E. coli*, at the highest peptide concentration, and after 2 h for *B. cereus*, at the highest KHS-Cnd tested against this bacterium.

It's noteworthy that the permeabilizing effects of KHS-Cnd were dose-dependent and time-dependent for both bacterial strains. However, to induce a strong perturbation of *B. cereus* plasmatic membrane, higher concentrations are needed compared to those that alter the outer membrane of *E. coli*. Interestingly, we observed a time-dependent reduction of extracellular protein content in the supernatants of bacterial cells treated with both concentrations of KHS-Cnd peptide. This could be due to a stronger effect of the peptide at the earliest time points tested; whereas at the longer ones, when the peptide starts to be degraded, the bacteria treated with KHS-Cnd were likely induced to counteract the alteration of peptidoglycan layer to strengthen the bacterial membrane. For this reason and to better understand the physiological perturbation induced by the KHS-Cnd peptide, we decided to investigate the metabolic extracellular footprints through ^{1}H NMR metabolomics analysis. Metabolites related to aminoacyl-tRNAs biosynthesis (Phe, Ala, Gly, Ser) and to peptidoglycan synthesis (N-acetylglucosamine) were found to be higher in *E. coli* supernatants particularly at 3 h after 3.0 μM KHS-Cnd treatment. The peptide exposure also determined relative higher levels of homocysteine in the bacterial culture supernatants, as well as of cystathionine, an intermediate of homocysteine synthesis pathway implicated in peptidoglycan synthesis. It's known that homocysteine is needed in the cell for *de novo* synthesis of methionine and, as a consequence, for the production of vital metabolic enzymes [28,29]. Thus, we can speculate that the excess of homocysteine being produced due to KHS-Cnd is not likely used for methionine production. On the other hand, acetate, that is a metabolite involved in energy-related pathway, had a lower concentration in *E. coli* supernatants after KHS-Cnd exposure at both incubation times. Some of our metabolomics results, in terms of relative metabolite concentrations changes, are in agreement with those obtained by Aries and colleagues (2020) due to *E. coli* grown in presence of a membrane disrupting agent like a multivalent quaternary ammonium functionalized macromolecule (DABCO), although in this paper intracellular differences were analysed [30].

Overall data of NMR metabolomics analysis revealed that *E. coli* supernatants contain components of peptidoglycan thus confirming the membranolytic activity of KHS-Cnd peptide. Furthermore, extracellular metabolic profiles highlighted potential changes in energy-related metabolites as a possible compensation effect whereby *E. coli* exposed to peptide likely consumes these metabolites to achieve the same bacterial density as the untreated control, as confirmed by comparable OD curves.

As for *B. cereus*, however, the analysis of extracellular metabolite profiles also confirmed that higher concentrations are necessary to induce alterations at metabolic level. Upon treatment with 6.0 μM KHS-Cnd peptide, in fact, the metabolic profiles of *B. cereus* were similar to those of the untreated control.

However, at the highest concentrations tested against *B. cereus*, betaine, involved in glycine and methionine metabolism [31], had lower levels in the supernatants of treated bacteria. Consequently, betaine would be expected to be converted and consumed to produce several metabolites such as serine, homocysteine, and methionine, whose levels, at least the extracellular ones, were lower in *B. cereus* treated with 12 μM KHS-Cnd compared to the control.

In contrast to *E. coli*, acetate had a higher concentration in *B. cereus* supernatants after exposure to 12 μM KHS-Cnd. This metabolite, whose accumulation in *B. cereus* medium and utilization during sporulation are well known, serves to provide a reducing potential for poly-β-hydroxybutyrate (PHB) synthesis [32,33]. On the other hand, we found that extracellular 2'-hidroxyisobutyrate levels were lower in treated bacteria that in untreated ones. However, we cannot exclude that, after depletion of acetate in the medium, PHB rapidly accumulates, thus providing carbon and energy source to counteract the peptide-induced metabolic alterations.

In addition to the membranolytic activity of KHS-Cnd peptide, this study highlights the potential of KHS-Cnd as an anti-virulence agent able to mitigate protease secretion, a key virulence factor produced by antibiotic-resistant pathogens. The current spread of antibiotic resistance demands alternative solutions in terms of new potential therapeutic targets and strategies. In this context, bacterial proteases, the largest family of enzymes in metabolism having key roles in cell viability, stress response and pathogenicity, offer an underexploited antimicrobial drug targets [34]. Nevertheless, to date, there are no protease inhibitors as antimicrobial agents in the clinic, except for the peptidoglycan biosynthetic transpeptidases sensitive to β-lactam antibiotics [35,36].

In conclusion, for a possible pharmaceutical application, we should also take into consideration our previous data available on its hemolytic activity against mammalian erythrocytes [16]. No hemolytic activity, a poor membranolytic activity and a slight or negligible cytotoxic effect were evidenced until a concentration of 5 μM, thus confirming the interesting potential of the peptide as a new drug especially for *E. coli* considering that already at 1.5 μM it exerts both membranolytic and anti-virulence activity on this bacterium.

CRediT authorship contribution statement

Esther Imperlini: Writing – review & editing, Writing – original draft, Investigation, Data curation. **Fernando Porcelli:** Writing – review & editing, Writing – original draft, Investigation, Data curation. **Stefano Borocci:** Writing – review & editing, Data curation, Conceptualization. **Francesco Buonocore:** Writing – review & editing, Supervision, Funding acquisition, Conceptualization. **Francesco Maiurano:** Methodology, Investigation, Data curation. **Anna Rita Taddei:** Methodology, Investigation, Data curation. **Federica Massaro:** Writing – original draft, Methodology, Investigation, Data curation. **Angelica Grifoni:** Methodology, Investigation, Data curation.

Declaration of Competing Interest

The authors have nothing to declare.

Acknowledgements

We acknowledge financial support under the National Recovery and Resilience Plan (NRRP), Mission 4, Component 2, Investment 1.1, Call for tender No. 104 published on 2.2.2022 by the Italian Ministry of University and Research (MUR), funded by the European Union – Next Generation EU – Project Title: Fish-inspired antimicrobial peptide delivered by specific nanosystems to fight ESKAPE bacteria: a powerful weapon against antibiotic resistance (code 2022FKLKSY) – CUP J53D23001090006.

Research project partially funded by Next Generation EU. Project code CN_00000033, Concession Decree No. 1034 of 17 June 2022 adopted by the Italian Ministry of University and Research, CUP J83C22000860007 (University of Tuscia) Project title "National Biodiversity Future Center – NBFC".

Appendix A. Supporting information

Supplementary data associated with this article can be found in the online version at doi:10.1016/j.peptides.2024.171311.

Data Availability

Data will be made available on request.

References

[1] L. Li, J. Ma, Z. Yu, M. Li, W. Zhang, H. Sun, Epidemiological characteristics and antibiotic resistance mechanisms of Streptococcus pneumoniae: an updated review, Microbiol Res 266 (2023) 127221.

[2] M. Radulescu, V. Gant, Gram-negative pulmonary infections - advances in epidemiology and diagnosis, Curr. Opin. Pulm. Med 29 (2023) 168–173.

[3] Y. Li, S. Kumar, L. Zhang, Mechanisms of antibiotic resistance and developments in therapeutic strategies to combat *Klebsiella pneumoniae* Infection, Infect. Drug Resist 17 (2024) 1107–1119.

[4] Y. Liu, J. Shi, Z. Tong, Y. Jia, B. Yang, Z. Wang, The revitalization of antimicrobial peptides in the resistance era, Pharm. Res 163 (2021) 105276.

[5] G. Satchanska, S. Davidova, A. Gergova, Diversity and mechanisms of action of plant, animal, and human antimicrobial peptides, Antibiot. (Basel) 13 (2024) 202.

[6] E. Piktel, U. Wnorowska, J. Gorbacz-Konończuk, J. Sienkiewicz, K. Głuszek, S. Okła, et al., From antimicrobial to anticancer: unraveling the potential of pleurocidin and pleurocidin-derived peptides in the treatment of cancers, Front Pharm. 15 (2024) 1340029.

[7] G.E. Valenti, S. Alfei, D. Caviglia, C. Domenicotti, B Marengo. Antimicrobial peptides and cationic nanoparticles: a broad-spectrum weapon to fight multi-drug resistance not only in bacteria, Int J. Mol. Sci. 23 (2022) 6108.

[8] H.X. Luong, T.T. Thanh, T.H. Tran, Antimicrobial peptides - advances in development of therapeutic applications, Life Sci. 260 (2020) 118407.

[9] P. Cardoso, H. Glossop, T.G. Meikle, A. Aburto-Medina, C.E. Conn, V. Sarojini, et al., Molecular engineering of antimicrobial peptides: microbial targets, peptide motifs and translation opportunities, Biophys. Rev. 13 (2021) 35–69.

[10] C. Zhang, M. Yang, Antimicrobial peptides: from design to clinical application, Antibiot. (Basel) 11 (2022) 349.

[11] Z. Jiang, A.I. Vasil, L. Gera, M.L. Vasil, R.S. Hodges, Rational design of α-helical antimicrobial peptides to target Gram-negative pathogens, *Acinetobacter baumannii* and *Pseudomonas aeruginosa*: utilization of charge, 'specificity determinants,' total hydrophobicity, hydrophobe type and location as design parameters to improve the therapeutic ratio, Chem. Biol. Drug Des. 77 (2011) 225–240.

[12] R.A.H. Bhat, D. Thakuria, R.S. Tandel, V.C. Khangembam, P. Dash, G. Tripathi, et al., Tools and techniques for rational designing of antimicrobial peptides for aquaculture, Fish. Shellfish Immunol. 127 (2022) 1033–1050.

[13] V. Rajanbabu, J.Y. Chen, Applications of antimicrobial peptides from fish and perspectives for the future, Peptides 32 (2011) 415–420.

[14] F. Buonocore, E. Randelli, D. Casani, S. Picchietti, M.C. Belardinelli, D. de Pascale, et al., A piscidin-like antimicrobial peptide from the icefish *Chionodraco hamatus* (Perciformes: Channichthyidae): molecular characterization, localization and bactericidal activity, Fish. Shellfish Immunol. 33 (2012) 1183–1191.

[15] C. Olivieri, F. Buonocore, S. Picchietti, A.R. Taddei, C. Bernini, G. Scapigliati, et al., Structure and membrane interactions of chionodracine, a piscidin-like antimicrobial peptide from the icefish *Chionodraco hamatus*, Biochim. Biophys. Acta 2015 (1848) 1285–1293.

[16] C. Olivieri, F. Bugli, G. Menchinelli, G. Veglia, F. Buonocore, G. Scapigliati, et al., Design and characterization of chionodracine-derived antimicrobial peptides with enhanced activity against drug-resistant human pathogens, RSC Adv. 8 (2018) 41331–41346.

[17] F. Buonocore, S. Picchietti, F. Porcelli, G. Della Pelle, C. Olivieri, E. Poerio, et al., Fish-derived antimicrobial peptides: activity of a chionodracine mutant against bacterial models and human bacterial pathogens, Dev. Comp. Immunol. 96 (2019) 9–17.

[18] M. Artini, E. Imperlini, F. Buonocore, M. Relucenti, F. Porcelli, O. Donfrancesco, et al., Anti-virulence potential of a chionodracine-derived peptide against multidrug-resistant *Pseudomonas aeruginosa* clinical isolates from cystic fibrosis patients, Int J. Mol. Sci. 23 (2022) 13494.

[19] F. Buonocore, P.R. Saraceni, A.R. Taddei, A. Miccoli, F. Porcelli, S. Borocci, et al., Antibacterial and anticancer activity of two NK-lysin-derived peptides from the Antarctic teleost Trematomus bernacchii, Fish. Shellfish Immunol. 142 (2023) 109099.

[20] E. Imperlini, C. Celia, A. Cevenini, A. Mandola, M. Raia, M. Fresta, et al., Nano-bio interface between human plasma and niosomes with different formulations indicates protein corona patterns for nanoparticle cell targeting and uptake, Nanoscale 13 (2021) 5251–5269.

[21] A.B. Schäfer, M.A. Wenzel, How-to guide for mode of action analysis of antimicrobial peptides, Front Cell Infect. Microbiol 10 (2020) 540898.

[22] M.W. Azam, R. Zarrilli, A.U. Khan, Updates on the virulence factors produced by multidrug-resistant enterobacterales and strategies to control their infections, Microorganisms 11 (2023) 1901.

[23] R.M. Raju, A.L. Goldberg, E.J. Rubin, Bacterial proteolytic complexes as therapeutic targets, Nat. Rev. Drug Discov. 11 (2012) 777–789.

[24] E. Culp, G.D. Wright, Bacterial proteases, untapped antimicrobial drug targets, J. Antibiot. (Tokyo) 70 (2017) 366–377.

[25] M.R. Loffredo, F. Savini, S. Bobone, B. Casciaro, H. Franzyk, M.L. Mangoni ML, et al., Inoculum effect of antimicrobial peptides, Proc. Natl. Acad. Sci. USA 118 (2021) e2014364118.

[26] D.K. Mercer, M.D.T. Torres, S.S. Duay, E. Lovie, L. Simpson, M. von Köckritz-Blickwede, et al., Antimicrobial susceptibility testing of antimicrobial peptides to better predict efficacy, Front Cell Infect. Microbiol 10 (2020) 326.

[27] J. Jovanovic, V.F.M. Ornelis, A. Madder, A. Rajkovic, *Bacillus cereus* food intoxication and toxicoinfection, Compr. Rev. Food Sci. Food Saf. 20 (2021) 3719–3761.

[28] N.L. Tuite, K.R. Fraser, C.P. O'byrne, Homocysteine toxicity in *Escherichia coli* is caused by a perturbation of branched-chain amino acid biosynthesis, J. Bacteriol. 187 (2005) 4362–4371.

[29] M. Walters, M.P. Sircili, V. Sperandio, AI-3 synthesis is not dependent on luxS in, *Escherichia coli*. J. Bacteriol. 188 (2006) 5668–5681.

[30] M.L. Aries, M.J. Cloninger, NMR metabolomic analysis of bacterial resistance pathways using multivalent quaternary ammonium functionalized macromolecules, Metabolomics 16 (2020) 82.

[31] M.L. Aries, M.J. Cloninger, NMR hydrophilic metabolomic analysis of bacterial resistance pathways using multivalent antimicrobials with challenged and unchallenged wild type and mutated gram-positive bacteria, Int J. Mol. Sci. 22 (2021) 13606.

[32] H.M. Nakata, Role of acetate in sporogenesis of *Bacillus cereus*, J. Bacteriol. 91 (1996) 784–788.

[33] H. Li, J. O'Hair, S. Thapa, S. Bhatti, S. Zhou, Y. Yang, et al., Proteome profile changes during poly-hydroxybutyrate intracellular mobilization in gram positive *Bacillus cereus* tsu1, BMC Microbiol 20 (2020) 122.

[34] E. Culp, G.D. Wright, Bacterial proteases, untapped antimicrobial drug targets, J. Antibiot. (Tokyo) 70 (2017) 366–377.

[35] K. Bush, P.A. Bradford, β-Lactams and β-lactamase inhibitors: an overview, Cold Spring Harb. Perspect. Med 6 (2016) a025247.

[36] J. Xuan, W. Feng, J. Wang, R. Wang, B. Zhang, L. Bo, et al., Antimicrobial peptides for combating drug-resistant bacterial infections, Drug Resist Updat 68 (2023) 100954.